Published OnlineFirst October 20, 2009; DOI: 10.1158/1541-7786.MCR-09-0187

UNC45A Confers Resistance to Histone Deacetylase Inhibitors and Retinoic Acid

Mirjam T. Epping,[1] Lars A.T. Meijer,[2] Johannes L. Bos,[2] and René Bernards[1]

[1]Division of Molecular Carcinogenesis, Centre for Biomedical Genetics and Cancer Genomics Centre, Netherlands Cancer Institute, Plesmanlaan 121, Amsterdam, the Netherlands and [2]Department of Physiological Chemistry, Centre for Biomedical Genetics and Cancer Genomics Centre, UMC Utrecht, Universiteitsweg 100, Utrecht, the Netherlands

Abstract

To identify potential biomarkers of therapy response, we have previously done a large-scale gain-of-function genetic screen to identify genes whose expression confers resistance to histone deacetylase inhibitors (HDACI). This genetic screen identified two genes with a role in retinoic acid signaling, suggesting that HDACIs target retinoic acid signaling as part of their anticancer effect. We study here a third gene identified in this genetic screen, *UNC45A*, and assess its role in retinoic acid signaling and responses to HDACIs using cell-based proliferation and differentiation assays and transcriptional reporter gene assays. The vertebrate *Unc45* genes are known for their roles in muscle development and the assembly and cochaperoning of the muscle motor protein myosin. Here, we report that human *UNC45A* (*GCUNC45*) can render transformed cells resistant to treatment with HDACIs. We show that UNC45A also inhibits signaling through the retinoic acid receptor α. Expression of UNC45A inhibits retinoic acid–induced proliferation arrest and differentiation of human neuroblastoma cells and inhibits the induction of endogenous retinoic acid receptor target genes. These data establish an unexpected role for UNC45A in causing resistance to both HDACI drugs and retinoic acid. Moreover, our data lend further support to the notion that HDACIs exert their anticancer effect, at least in part, through an effect on retinoic acid signaling. (Mol Cancer Res 2009;7(11):1861–70)

Introduction

The evolutionarily highly conserved *Unc45*-like genes are involved in muscle development and in the assembly of the motor protein myosin (1). The *C. elegans unc-45* locus encodes a single Unc45 protein. A genetic analysis of *unc-45* has revealed recessive lethal alleles, demonstrating that Unc45 function is essential to *C. elegans* development (2). Vertebrate genomes contain two differential *Unc45* genes, which are located on different chromosomes. Human *UNC45A* (15q26.1) has also been called general cell *GCUNC45* or smooth-muscle cell–associated protein-1 (*SMAP-1*) and is ubiquitously expressed, whereas the expression of *UNC45B* (chr. 17q12) is restricted to striated muscle (3). UNC45A and B are quite different from one another with only 55% to 56% identity and 74% similarity in amino acid sequence, but the orthologs are up to 94% identical between mouse and man (3).

Unc45 proteins contain an NH_2-terminal tetratricopeptide repeat domain, a central region, and a COOH-terminal domain named UCS after the founding members of the family (*C. elegans Unc-45*; *P. anserine Cro1*; *S. cerevisiae She4p*; refs. 1, 4). This three-domain configuration is maintained in all animal Unc45 proteins identified. The Unc45 tetratricopeptide repeat domain binds the molecular chaperone Hsp90 in a stoichiometric manner. The UCS domain binds myosin and shows molecular chaperone activity with the myosin head (5). Mutations in *C. elegans unc-45* result in paralysis due to disruption of myosin assembly in the thick filaments of body wall muscle cells (1). The protein encoded by the zebrafish gene *Unc-45b/Steif* interacts physically and functionally with Hsp90a and is required for motility and myofibrillogenesis (6, 7). *C. elegans* Unc45 is regulated by multiubiquitylation by the E3/E4 complex Chn-1/Ufd-2 (8). Transgenic nematodes overexpressing *Unc45* also display defects in myosin assembly, with decreased myosin content and a mild paralysis phenotype. The reduced myosin accumulation is a result of myosin degradation through the ubiquitin/proteasome system (9).

Unc45A and B seem to have distinct functions in muscle cell differentiation. The expression of *Unc45A* decreases, whereas *Unc45B* expression increases during muscle differentiation in mouse C2C12 myoblasts. In these cells, *Unc45A* antisense inhibited cell proliferation and myoblast fusion, but *Unc45B* antisense reduced fusion to a lesser extent and affected sarcomere formation more directly (3). UNC45A is the first HSP90 cochaperone to show α/β isoform specificity, as it shows selectivity for HSP90β (10).

UNC45A has recently been described as a modulator of the molecular chaperoning of progesterone receptor (PR) by HSP90 (11). By inhibiting the ATPase activity of HSP90, UNC45A blocks the chaperoning of PR to its hormone-binding state (11).

The expression of UNC45A protein in ovarian carcinoma is associated with tumor stage and grade (12). Malignant serous

Received 5/5/09; revised 8/28/09; accepted 8/28/09; published OnlineFirst 10/20/09.
Grant support: Netherlands Genomics Initiative/Netherlands Organization for Scientific Research, the Netherlands Proteomics Centre, and the Dutch Cancer Society.
The costs of publication of this article were defrayed in part by the payment of page charges. This article must therefore be hereby marked *advertisement* in accordance with 18 U.S.C. Section 1734 solely to indicate this fact.
Note: Supplementary data for this article are available at Molecular Cancer Research Online (http://mcr.aacrjournals.org/).
Requests for reprints: René Bernards, Netherlands Cancer Institute, Division of Molecular Carcinogenesis B7, Plesmanlaan 121, 1066 CX Amsterdam, the Netherlands. Phone: 31-205-121952; Fax: 011-31-205-121954. E-mail: r.bernards@nki.nl

doi:10.1158/1541-7786.MCR-09-0187

Published OnlineFirst October 20, 2009; DOI: 10.1158/1541-7786.MCR-09-0187

carcinoma expresses elevated levels of UNC45A compared with normal ovarian surface epithelium and benign cysts (12). Furthermore, UNC45A colocalizes with myosin II at the cleavage furrow during cytokinesis and affects cell proliferation and motility (12).

Gene activity is regulated by many genetic and epigenetic factors, including the acetylation status of nucleosomal histone proteins. Histone acetylases catalyze the addition of acetyl groups to histones, whereas histone deacetylases (HDAC) remove these moieties. Small-molecule inhibitors of HDACs show tumor cell–selective cytotoxic activity and have potential as anticancer drugs (13).

Previously, we have conducted a functional genetic screen to identify genes that could render cells resistant to HDAC inhibitors (HDACI; ref. 14). One of the genes identified in this screen was UNC45A. In the present report, we have further investigated the function of human UNC45A in mammalian cells and we describe an unexpected role for UNC45A as an inhibitor of retinoic acid (RA) signaling.

Results

Expression of UNC45A Provides Resistance to HDACI

To identify genes involved in resistance to HDACIs, we have previously conducted a genetic screen, which revealed a role for the RA signaling pathway as a target of this group of drugs (14, 15). Briefly, in this genetic screen, *p53*-deficient mouse embryonic fibroblasts (MEF) containing an activated Ras^{V12} (Ras^{V12} MEFs) were transduced with a human cDNA expression library. The cells were then exposed to the hydroxamate HDACI PXD101 (belinostat) to induce cell cycle arrest and apoptosis. Drug-resistant cells formed colonies, which were picked to identify the proviral cDNAs inserts that had caused HDACI resistance. We identified two cancer-associated genes which, when overexpressed, could rescue the cells from the growth arrest imposed by HDACI treatment: RA receptor α (*RARα*) and preferentially expressed antigen in melanoma (*PRAME*), a repressor of RA signaling (14, 16). This finding implicated a rate-limiting role for RA signaling in the cytotoxic effects of HDACI (14).

Further analysis of the cDNAs present in PXD101-resistant colonies from this genetic screen revealed one more candidate HDACI-resistance gene: a partial cDNA corresponding to human UNC45A. This clone encompassed amino acids 365 to 929 of UNC45A/SMAP-1 (isoform 2) with the first internal ATG in this sequence being a methionine at position 424. Therefore, this clone would be translated into an NH_2-terminal truncated protein, denoted as ΔN-UNC45A (424-929). We cloned the full-length, wild-type UNC45A cDNA and tested if UNC45A could mediate resistance to HDACI in *p53*-deficient Ras^{V12} MEFs. After infection with retroviral UNC45A, RARα (used as a positive control) and green fluorescent protein (GFP; used as a negative control), Ras^{V12} MEFs were plated at clonal density and cultured in the continuous presence of PXD101. Infection of the cells with retroviral vectors encoding UNC45A and RARα resulted in resistance to PXD101 as measured by colony outgrowth, whereas the GFP-infected cells were growth-arrested (Fig. 1A). A specific antibody against UNC45A detected the ectopic UNC45A and an antibody against RARα detected the endogenous and ectopic RARα in lysates of the Ras^{V12} MEFs (Fig. 1B). Treatment with PXD101 induced an increase in $p21^{CIP}$ protein levels and increases in histone H3 and H4 acetylation, but these were not affected by the ectopic expression of either UNC45A or RARα, indicating that UNC45A acts downstream of histone acetylation to bypass the HDACI-induced cytostatic effect (Fig. 1B). Ras^{V12} MEFs primarily responded to PXD101 by proliferation arrest, which preceded apoptosis. Caspase-dependent apoptosis was activated in PXD101-treated cells as shown by the cleavage of poly ADP ribose polymerase. No differences in poly ADP ribose polymerase cleavage were apparent between Ras^{V12} MEFs expressing GFP, RARα, or UNC45A, indicating that apoptosis was not impaired in these cells (Supplementary Fig. S4). We also tested if Bcl-2, a major regulator of apoptosis, was changed upon treatment with PXD101. Although there were no differences in Bcl-2 levels between Ras^{V12} MEFs with GFP, RARα, or UNC45A, we noticed that Bcl-2 levels were moderately elevated in PXD101-resistant RARα and UNC45A colonies, most likely as a result of the selection pressure imposed by the continuous HDACI treatment (Supplementary Fig. S4).

As shown previously, treatment with HDACI induces RA signaling, which can be inhibited by overexpression of RARα and PRAME (14). To test if UNC45A also affected RA signaling, we used a reporter construct containing three RA-responsive elements (RARE) fused to luciferase (RARE-luc). This reporter was activated by PXD101 and by suberoylanilide hydroxamic acid (vorinostat), as well as by an HDACI from another chemical family, the benzamide HDACI MS-275. However, coexpression of UNC45A inhibited the activation of this reporter by either HDACI (Fig. 1C). Therefore, UNC45A may confer resistance to PXD101 by restoring repression of RA-responsive loci, similar to RARα and PRAME (14). Hence, we hypothesized that UNC45A may act as a negative modulator of RA signaling.

Repression of Nuclear Hormone Receptor Signaling by UNC45A

To test if UNC45A affects RA signaling, we cotransfected the RARE-luc reporter and UNC45A or ΔN-UNC45A in U2OS cells before treating them with all-*trans* RA (ATRA). Treatment with ATRA induced activation of the reporter, which was inhibited by the coexpressed ΔN-UNC45A (Fig. 2A). Moreover, full-length UNC45A imposed an even better inhibition of ATRA-induced reporter activation than ΔN-UNC45A (Fig. 2A). When 9-*cis*-RA was used as a ligand to induce RA signaling, a similar inhibition of reporter activity by UNC45A was found (Fig. 2B). A mammalian two-hybrid assay confirmed the existence of the interaction between RARα and its obligate heterodimerization partner RXRα in the presence of UNC45A. A Gal4-RARα fusion construct together with a VP16-RXRα construct mediated strong activation of a Gal4-driven luciferase reporter upon addition of ATRA or 9-*cis*-RA. This activation was of similar strength both in the presence and absence of UNC45A, indicating that the RARα-RXRα dimer was not perturbed by UNC45A (Fig. 2D). To test if UNC45A inhibited RARα-dependent transactivation per se, we expressed Gal4-RARα in the presence and absence of UNC45A, together with a GAL4-responsive reporter gene construct. As expected, treatment of the cells with ATRA induced

Published OnlineFirst October 20, 2009; DOI: 10.1158/1541-7786.MCR-09-0187

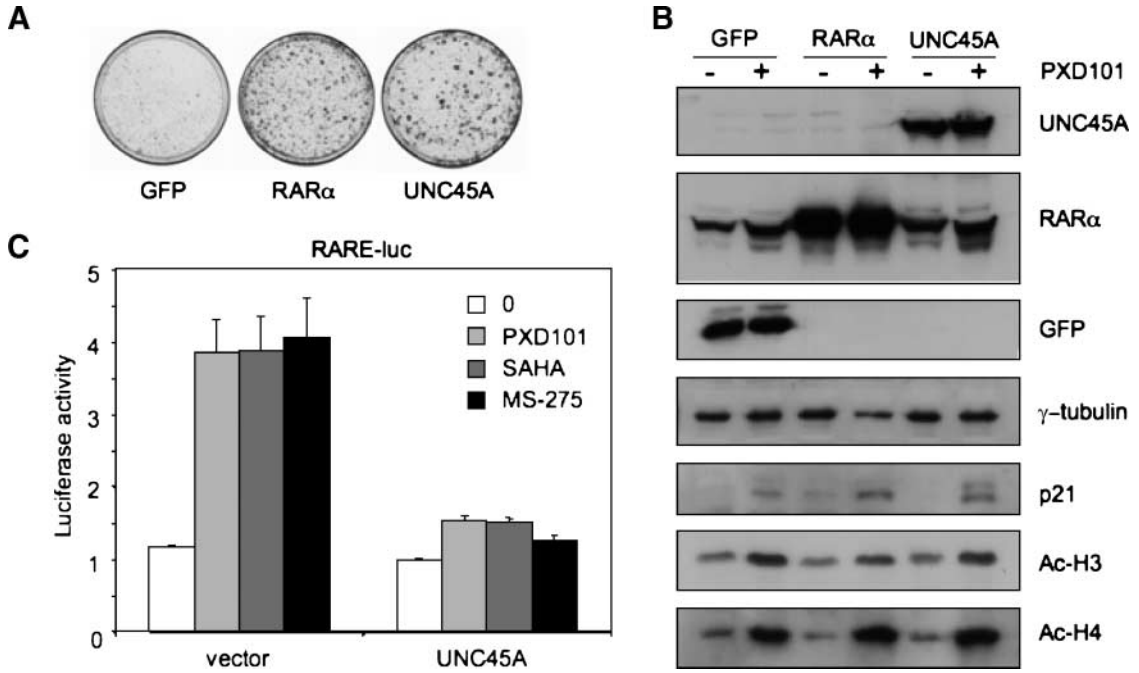

FIGURE 1. UNC45A expression provides resistance to HDACIs. **A.** A functional genetic screen for HDACI resistance genes identified UNC45A as a gene that could render Ras^{V12} MEFs resistant to the growth arrest and apoptosis induced by PXD101 (14). In a colony formation assay, Ras^{V12} MEFs were infected with retroviruses encoding for GFP, RARα, or UNC45A, plated at low density, and selected in PXD101 (1 μmol/L) for 3 wk. **B.** Immunoblot showing GFP, RARα, and UNC45A protein levels in Ras^{V12} MEFs upon retroviral infection. The cells were treated with PXD101 (1 μmol/L) for 16 h, and in cell extracts, the levels of p21 and acetylated histone H3 and H4 were determined. **C.** U2OS cells were transfected with RARE3-TK-luc and UNC45A and treated with PXD101 (2 μmol/L), suberoylanilide hydroxamic acid (*SAHA*; 2 μmol/L), or MS-275 (2 μmol/L).

activation of the Gal4-luc reporter in the absence of UNC45A, but in the presence of UNC45A, Gal4-RARα–mediated transactivation was significantly inhibited (Fig. 2C).

Subsequently, we tested if UNC45A could modulate signaling through any of the other class I and class II nuclear hormone receptors by using specific luciferase reporters. We found that UNC45A could inhibit PR signaling and ligand-dependent transactivation of both peroxisome proliferator-activated receptor (PPAR) α and γ, but did not have a significant effect on estrogen receptor signaling (Fig. 3A–D). PRAME did not confer detectable repression of PPAR signaling, as shown before (16).

Unc45A is ubiquitously expressed, whereas *Unc45B* is only expressed in striated muscle cells (3). We subjected a series of human tumor cell lines to an analysis of UNC45A protein levels and found that all tumor cell lines tested expressed UNC45A, although the protein levels varied between the cell lines (Supplementary Fig. S1). These data confirm the ubiquitous expression pattern of UNC45A. To test if inhibition of UNC45A would sensitize cells to HDACI treatment, we used siRNAs that effectively reduced the endogenous UNC45A protein levels (Supplementary Fig. S4). MCF7 breast carcinoma cells, among other cell lines, contained high UNC45A levels, but knockdown of UNC45A did not significantly modify the sensitivity of MCF7 cells to PXD101. This indicates that the endogenous levels of UNC45A in these tumor cells are not rate limiting for HDACI-induced growth arrest and is in line with the notion that there are many factors that affect sensitivity to HDACIs (15).

To identify proteins that associate *in vivo* with UNC45A, we affinity purified UNC45A from U2OS cells and subjected the UNC45A immunoprecipitates to mass spectrometry analysis. Among the proteins that coprecipitated with UNC45A were myosin and HSP90, but our analysis did not reveal new interactors of UNC45A (Supplementary Fig. S2). Myosin and HSP90 have been identified before to interact both genetically and physically with UNC45A and our experiments confirmed their associations with UNC45A (5). No phosphorylated species of UNC45A were identified, providing no evidence for regulation of UNC45A by phosphorylation.

Nuclear receptor coregulators frequently contain leucine-rich nuclear receptor boxes, LXXLL motifs, which mediate their interactions with nuclear hormone receptors (17, 18). UNC45A contains four such motifs, whereas in ΔN-UNC45A, only the two COOH-terminal nuclear receptor motifs are present (Fig. 4A). We generated mutants of each of these motifs by changing leucines to alanines, which allowed us to ask if these motifs are important for the inhibition of RA signaling. However, when wild-type and mutant UNC45A were compared, the nuclear receptor box mutants of UNC45A inhibited RA signaling to a similar extent as did wild-type UNC45A, indicating that each of these motifs are individually not required for the observed interference with RA signaling (Fig. 4D).

UNC45A Inhibits Differentiation and Growth Arrest Induced by ATRA

Neuroblastoma cells often show proliferation arrest and morphologic differentiation upon treatment with ATRA (19,

Published OnlineFirst October 20, 2009; DOI: 10.1158/1541-7786.MCR-09-0187

20). Clinical trials showed that ATRA treatment after completion of intensive chemoradiotherapy significantly improved survival in high-risk neuroblastoma patients (21, 22). We investigated whether UNC45A can modulate the effects of ATRA on human neuroblastoma cell lines. Human SK-N-BE neuroblastoma cells are sensitive to ATRA and were effectively growth arrested when cultured in medium containing ATRA. Ectopic expression of UNC45A allowed continuous proliferation of the cells the presence of ATRA, whereas GFP-expressing control cells were arrested (Fig. 5A–C). RAR-R4 is a RARα mutant that is a constitutive repressor of RA signaling due to its inability to bind ligand. SK-N-BE cells expressing RAR-R4 were used as positive controls and were completely resistant to ATRA (Fig. 5A–C). The UNC45A protein levels required for resistance to ATRA were similar to UNC45A levels in several cancer cell lines (Fig. 5D). Neither the endogenous nor the ectopically expressed UNC45A protein levels were affected by treatment with ATRA (data not shown).

Similarly, IMR32 neuroblastoma cell lines exhibited proliferation arrest in response to ATRA, but expression of UNC45A prevented this arrest (Supplementary Fig. S3). Again, the UNC45A protein levels required for the resistance against ATRA-induced proliferation arrest were similar to the endogenous UNC45A levels in various human cancer cell lines (Supplementary Fig. S3).

We also tested if UNC45A expression could affect differentiation induced by ATRA in one of the most well-defined models for ATRA-induced differentiation: F9 embryonic carcinoma cells. These cells differentiate to primitive endoderm upon treatment with ATRA. The expression of UNC45A inhibited the differentiation of cells cultured in ATRA and these cells grew out to form colonies with concomitant morphologic changes (Supplementary Fig. S3). UNC45A did not affect cell growth or morphology in the absence of ATRA. Ectopic expression of RAR-R4 in F9 resulted in resistance to ATRA-mediated differentiation, as expected (Supplementary Fig. S3).

To further substantiate the effects of UNC45A on ATRA-induced growth arrest and differentiation in human neuroblastoma, we expressed UNC45A in the frequently studied human SH-SY-5Y neuroblastoma cell line. In the absence of ATRA, UNC45A did not alter the proliferation and morphology of the cells. Treatment with ATRA inhibited the growth of control SH-SY-5Y cells, whereas cells expressing UNC45A continued to proliferate (Fig. 6A and B). The growth rates of cells expressing RAR-R4 were not affected by ATRA and these cells were completely resistant to ATRA (Fig. 6A and B). We also expressed the UNC45A nuclear receptor box mutants in SH-SY-5Y cells and verified their equal expression (Fig. 4C). Cells expressing the UNC45A mutants proliferated at similar rates to cells expressing wild-type UNC45A in the presence and absence of ATRA, indicating that the nuclear receptor boxes were not required for cellular resistance to ATRA (Fig. 4B).

To assess if UNC45A could modulate the effects mediated by activation of RXR, we used an RXR-specific ligand, LGD1069 (bexarotene). Treatment with LGD1069 attenuated the growth rates of SH-SY-5Y cells, but UNC45A provided resistance to RXR-mediated proliferation arrest (Fig. 6C). SH-SY-5Y cells with ectopic UNC45A were also resistant to

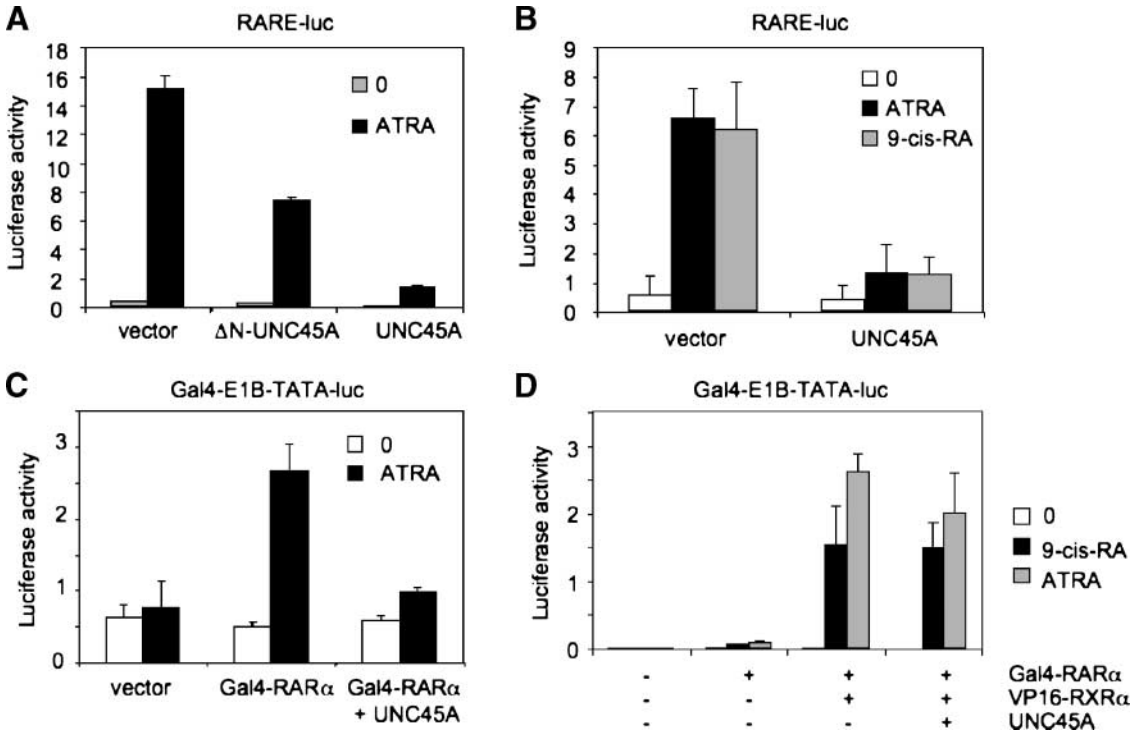

FIGURE 2. UNC45A inhibits RA signaling. **A** and **B.** U2OS cells were transfected with RARE3-TK-luc and UNC45A or ΔN-UNC45A followed by treatment with ATRA or 9-*cis*-RA. **C.** Luciferase reporter assay showing the inhibitory effects of UNC45A on Gal4-RARα–mediated transactivation. **D.** In a mammalian two-hybrid assay, Gal4-RARα and VP16-RXRα fusion proteins were cotransfected in the absence or presence of an UNC45A expression vector.

Published OnlineFirst October 20, 2009; DOI: 10.1158/1541-7786.MCR-09-0187

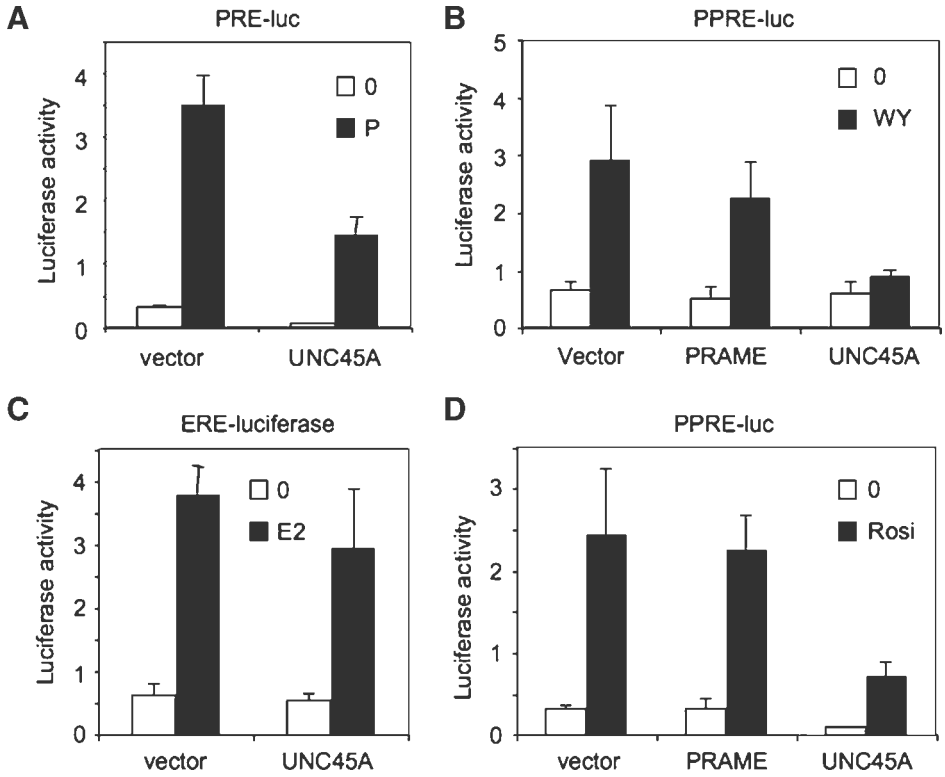

FIGURE 3. UNC45A inhibits progesterone and PPAR signaling. **A** and **C.** Cells were cotransfected with luciferase reporters containing either progesterone- or estrogen-responsive elements (PRE-luc or ERE-luc, respectively) and their corresponding receptors. The cells were treated with 1 μmol/L progesterone (*P*) or estradiol (*E2*). **B** and **D.** Cells were cotransfected with a luciferase reporter with PPAR-responsive elements (PPRE3-TK-luc) and either PPARα (**B**) or PPARγ (**D**). The cells were treated with 1 μmol/L of the synthetic PPAR ligands WY-14643 (*WY*) for PPARα and rosiglitizone (*Rosi*) for PPARγ.

growth arrest imposed by treatment with PXD101 (Supplementary Fig. S4).

Treatment with ATRA induces a change in gene expression patterns in responsive cells, which results in cell cycle arrest and differentiation. We analyzed the mRNA levels of *bona fide* RA target genes, *RARβ* and *CRABP2*, in SH-SY-5Y cell treated with ATRA. The transcript levels of these genes were induced by ATRA, whereas UNC45A significantly attenuated the induction of *RARβ* and *CRABP2* (Fig. 7A and B).

To address whether UNC45A interfered with neuroblastoma differentiation, we examined the expression of several critical neural differentiation markers: the neurotrophic receptor TRKB and the receptor for the glial cell–derived neurotrophic factor, RET. It has been shown that expression of these receptor kinases is induced upon ATRA treatment and these receptors are causally involved in ATRA-induced differentiation in neuroblastoma cells in culture (23-25). When the control SH-SY-5Y cells were exposed to ATRA for 3 weeks, the mRNA levels of *TRKB* (*NTRK2*) and *RET* were induced (Fig. 7C and D). In contrast, the induction of these neurotrophic receptors in cells expressing UNC45A and RAR-R4 was significantly inhibited (Fig. 7C and D).

Discussion

We have recently reported the results of a genetic screen in which we searched for genes whose ectopic expression interfered with the anticancer effects of HDACIs. This initial screen identified two known components of RA signaling, RARα and PRAME (14). In the present report, we have analyzed a third gene found in the genetic screen, *UNC45A*. *UNC45A* acted in a similar manner as the other two genes identified: overexpression of UNC45A rendered cells resistant to growth arrest induced by HDACIs and inhibited RAR-dependent *trans*-activation induced by HDACIs and retinoids. Thus, the genetic screen identified three genes that can mediate resistance to HDACIs, all of which act in the RA signaling pathway. This provides support to the notion that HDACIs act, at least in part, through derepression of RA signaling to inhibit cancer cell growth (14). In line with this notion, combined treatment with HDACIs and retinoids strongly enhances RA signaling, and in preclinical *in vivo* models, cooperative effects of retinoids and HDACIs on tumor growth inhibition have been observed, for example, in renal cell carcinoma and neuroblastoma (14, 26, 27).

UNC45A inhibited ATRA-induced differentiation and growth arrest in various ATRA-sensitive cell types. Given that Unc45-like proteins have mainly been known as cochaperones and assembly factors for myosin, our finding that UNC45A can act as an inhibitor of RA signaling and RA-induced proliferation arrest and differentiation indicates that the function of UNC45A in mammalian cells may not be limited to myosin cochaperoning.

We observed an inhibition of RAR-, PR- and PPAR-dependent *trans*-activation upon ectopic expression of *UNC45A*. Recently, UNC45A has been shown to modulate the chaperoning of PR through binding to and inhibiting the ATPase activity of HSP90 (11). Our efforts to identify previously unrecognized proteins that physically interact with UNC45A did not reveal any proteins other than the known myosin and HSP90 (ref. 5, Supplementary

Published OnlineFirst October 20, 2009; DOI: 10.1158/1541-7786.MCR-09-0187

Fig. 2). Therefore, it is at present unclear through which mechanism UNC45A inhibits RA signaling. UNC45A contains four putative nuclear receptor boxes, small leucine-rich motifs, which mediate the interactions of coregulators with nuclear hormone receptors (17, 18). In spite of this, we have not observed a direct physical interaction between RARα and UNC45A (data not shown). The nuclear receptor boxes in UNC45A were individually not required for inhibition of RA-induced proliferation arrest. Similarly, these motifs have been shown to be nonessential for the role of UNC45A in PR chaperoning (11).

Recently, elevated UNC45A levels have been detected in serous ovarian carcinomas biopsies and UNC45A was found to affect cell proliferation and motility (12). Our data provide a second explanation for the increased UNC45A levels in cancer, as high UNC45A may provide a selective advantage to tumor cells by inhibition of RA-dependent proliferation arrest and differentiation. Hence, in addition to its proposed role in ovarian carcinoma, UNC45A may play a role in other cancers, either through affecting motility or by attenuating RA signaling.

Materials and Methods

Plasmids, Reagents, and Antibodies

The ΔN-UNC45A–truncated cDNA was generated by PCR using genomic DNA from PXD101-resistent RAS^{V12} MEFs as the template. These PXD101-resistant cells had been generated in a functional genetic screen, as described previously (14). ΔN-UNC45A was cloned into the pcDNA3.1 expression vector and the pMX retroviral expression vector. Full-length UNC45A was made by PCR from pooled plasmid DNA of a human erythroleukemia K562 cDNA library and cloned into the pCR3-CMV-flag expression vector and the MSCVpuro retroviral vector. The RARα, RAR-R4 and PRAME constructs, the expression vectors for nuclear hormone receptors, and the luciferase reporters have been described before (14, 16). UNC45A mutants were generated by site-directed mutagenesis PCR and cloned into pCR3-CMV-flag and pBabePuro. ATRA, 9-*cis*-RA, MS-275, β-estradiol, progesterone, WY-14643, and rosiglitizone were purchased from SIGMA, PXD101 (belinostat) was a gift from Topotarget/Prolifix Ltd, and LGD1069 (bexarotene) was purchased from LCLabs. The UNC45A siRNA pool was

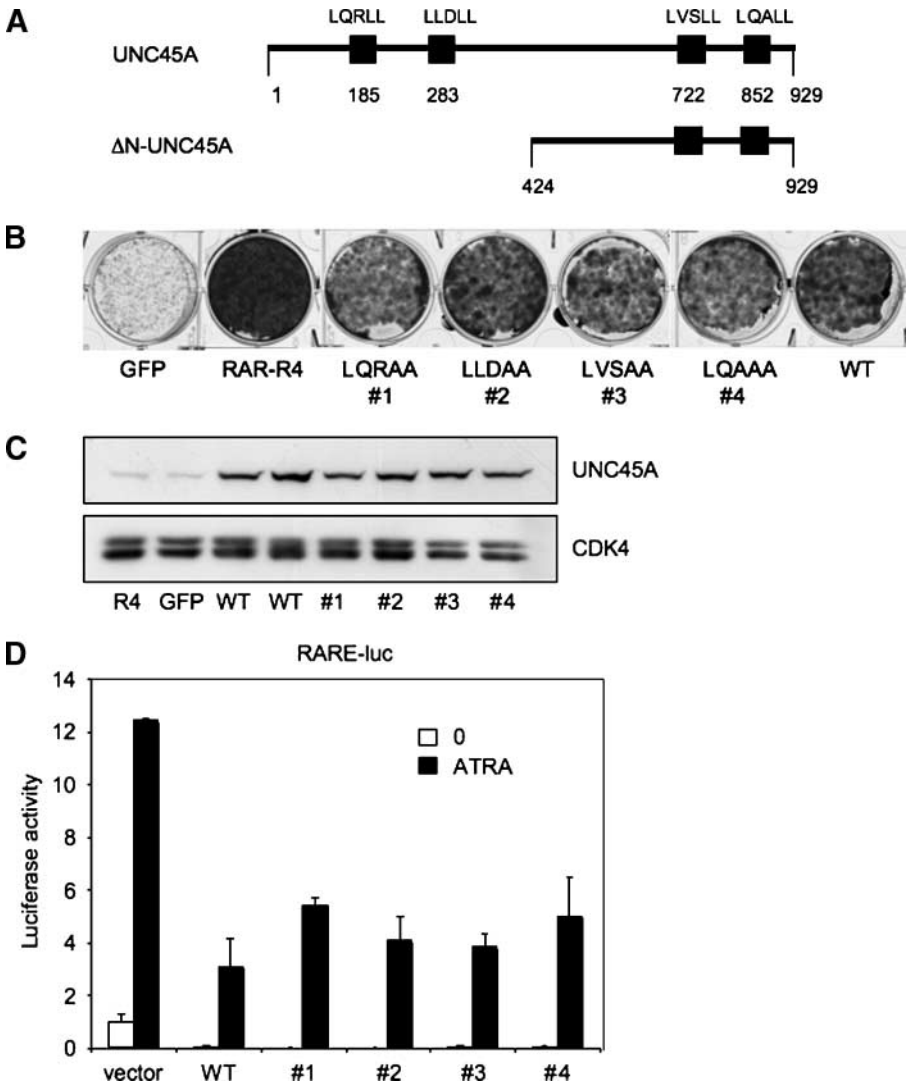

FIGURE 4. Nuclear receptor box motifs in UNC45A. **A.** Schematic representation of UNC45A and the NH_2-terminally truncated UNC45A clone identified in the functional genetic screen. The nuclear receptor boxes are indicated with amino acid numbering according to the sequence of UNC45A isoform 2/SMAP-1. **B.** UNC45A nuclear receptor box mutants were generated by changing leucines to alanines, resulting in the indicated mutant sequences. SH-SY-5Y cells were infected with retroviruses encoding wild-type (*WT*) and mutant UNC45A and cultured in the presence of 0.1 μmol/L ATRA. **C.** Immunoblot showing equal expression of wild-type and mutant UNC45A in SH-SY-5Y cells. CDK4 was used as a loading control. **D.** U2OS cells were cotransfected with RARE3-TK-luc and wild-type and mutant UNC45A before treatment with ATRA (1 μmol/L).

Published OnlineFirst October 20, 2009; DOI: 10.1158/1541-7786.MCR-09-0187

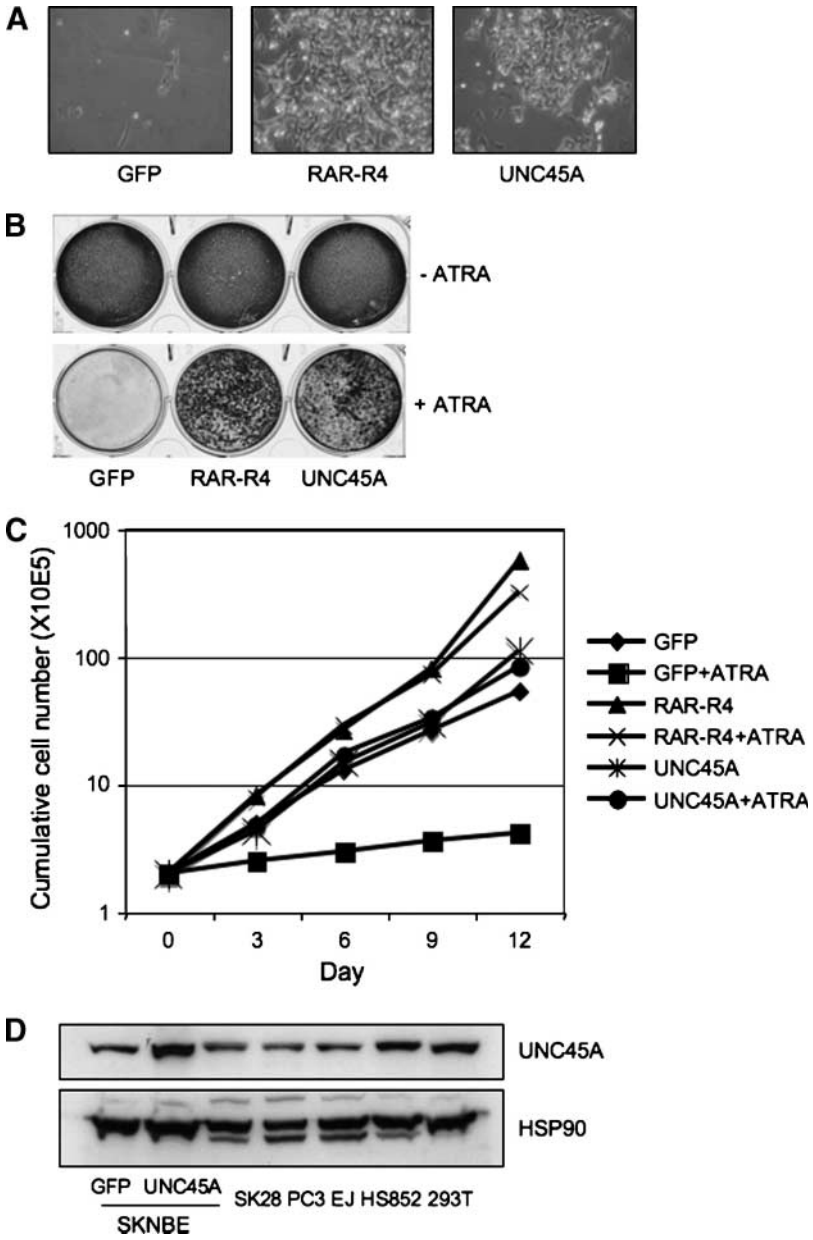

FIGURE 5. UNC45A inhibits proliferation arrest induced by ATRA. **A** and **B.** SK-N-BE cells were infected with GFP, RAR-R4, or UNC45A and cultured in ATRA (0.1 μmol/L). The cells were stained and dishes were photographed (×400) after 3 wk. **C.** Proliferation of SK-N-BE cells (± ATRA) was determined by counting cell numbers every 3rd day. **D.** Immunoblot showing the UNC45A protein levels in SK-N-BE cells expressing UNC45A or GFP compared with several human tumor cell lines.

purchased from Dharmacon and contained these sequences: 1. CUAUAUAAGUGCAGCGAGAUU; 2. UUCAGGAGAAGGUGCGAUAUU; 3. CAGUGGAGCAGCUGCGGAAUU; and 4. GCUAAGCAGUGUCGAAAGUUU. Anti-UNC45A affinity-purified antibodies were generated by immunizing rabbits with the peptides AKQHVPEQHPKDKPS and CHLKLEDYDKAETEAS. Antibodies against RARα (C-20), $p21^{CIP}$ (F5), GFP (FL), CDK4 (C-22), HSP90α/β (H-114), Bcl-2 (C-2), and γ-tubulin (H-183) were from Santa Cruz Biotechnology. The poly ADP ribose polymerase antibody (46D11) was from Cell Signaling and the β-actin antibody was from Sigma. Antibodies against acetylated-H3 and H4 were from Serotec and Upstate Biotechnology, respectively.

Cell Culture, Colony Formation, and Differentiation Assays

All cells were cultured in DMEM supplemented with 10% FCS. RAS^{V12} MEFs were generated by infection of p53−/− MEFs with a pBabePuro-Ras^{V12} retrovirus. Retroviral supernatants were generated by transfection of Phoenix packaging cells with retroviral plasmids. For colony formation assays, RAS^{V12} MEFs were infected with the indicated viruses and seeded at a cell density of 5×10^4 cells/10-cm tissue culture dish 48 h after infection. PXD101 (1 μmol/L) was added to the medium 16 h after plating, and fresh medium with PXD101 was added every third day. Dishes were stained with Coomassie blue 14 to 18 d after plating. For differentiation assays, F9 cells were infected with UNC45A retrovirus (MSCV-EGFP-pgk-UNC45A-ires-puro,

Published OnlineFirst October 20, 2009; DOI: 10.1158/1541-7786.MCR-09-0187

a derivative of MSCVpuro), selected in puromycin, seeded at a density of 10,000 cells/10 cm^2, and cultured in 1 μmol/L ATRA for 48 h. The cells were then detached, diluted 1:10 to 1:20, and replated (10 cm^2) and cultured in 1 μmol/L ATRA for another 14 d. Neuroblastoma cells were infected with MSCV-UNC45A, MSCV-GFP, or MSCV-RAR-R4 retroviral supernatants, seeded at a density of 10,000 cells/10 cm^2, and cultured in ATRA or LGD1069. The cells cultured in LGD1069 were diluted 1:5 and replated in medium containing LGD1069 after 9 d.

Transfections and Luciferase Assays

U2OS cells were cultured in DMEM supplemented with charcoal/dextran-treated FCS (Hyclone) and transfected with 0.5 μg of reporter-luciferase, 10 ng CMV-renilla, and 3 μg of the indicated expression plasmids using calcium phosphate precipitation. The indicated ligands (1 μmol/L unless otherwise indicated) were added 48 h after transfection and assays were done 72 h after transfection. Normalized luciferase activities shown represent ratios (mean ± SD of triplicates) between luciferase values and renilla internal control values and were measured using the dual reporter luciferase assay system (Promega).

Quantitative Reverse Transcription-PCR

Quantitative reverse transcription-PCR assays were carried out to measure mRNA levels of genes using the 7500 Fast Real-Time PCR System as described (28). Relative mRNA levels of each gene shown were normalized to the expression of the housekeeping gene *GAPDH*. Quantitative PCR reactions were done using the SYBR Green master mix (Applied Biosystems). The sequences of the primers were as follows: RARβ fwd TGAGTCCTGGGCAAATCCTG and rev CGGTTTGGGTCAATCCACTGA; CRABP2 fwd TCGGAAAACTTCGAGGAATTGC and rev CCTGTTTGATCTCCACTGCTG; TRKB fwd: TGTTCAGCACATCAAGCGACA and rev CAAAGGCTCCTTCGCCTAGC; RET fwd GGCATCAACGTCCAGTACAAG and rev TGAGGTGACCACCCCTAGC; glyceraldehyde-3-phosphate dehydrogenase fwd AAGGTGAAGGTCGGAGTCAA and rev: AATGAAGGGGTCATTGATGG.

Western Blotting

Cells were lysed in RIPA buffer [50 mmol/L Tris (pH 8.0), 150 mmol/L NaCl, 1% NP40, 0.5% deoxycholic acid, and 0.1% SDS] supplemented with protease inhibitors (Complete; Roche) and proteins were separated on 10% to 12% SDS-PAGE gels. Proteins were transferred to polyvinylidine difluoride membranes (Immobilon P, Millipore) and the blots were probed with the indicated antibodies.

Protein Purification and Mass Spectrometry

The pBabePuro retroviral vector was modified to express NH2-terminal tags to allow tandem affinity purification of UNC45A. The biotinyl tag MASSLRQILDSQKMEWRSNAGGS (29) was cloned into pBabePuro and three flag tags were added to the BamHI site upstream of the biotinyl tag. UNC45A was cloned into the EcoRI site downstream of the tags, resulting in the pBabePuro-3Xflag-Nbio-UNC45A retroviral plasmid. The BirA biotin ligase was cloned into MSCVneo. U2OS cells were infected with the UNC45A retrovirus and selected in 2 μg/mL puromycin, and subsequently infected with the MSCVneo-BirA retrovirus and selected in 2 mg/mL neomycin. To immunoprecipitate UNC45A, the

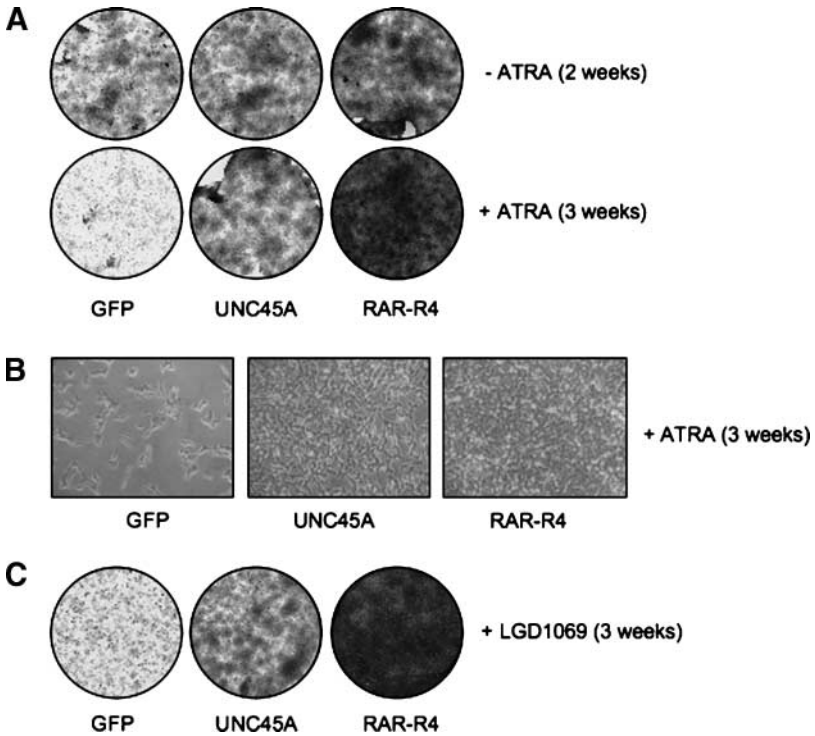

FIGURE 6. UNC45A inhibits ATRA-induced differentiation. **A** and **B.** SH-SY-5Y cells were infected with GFP, RAR-R4, or UNC45A and cultured in ATRA (0.1 μmol/L) to allow for differentiation and growth arrest to occur. Cells were photographed (×400) and dishes were stained after 2 to 3 wk. **C.** SH-SY-5Y cells were infected with GFP, RAR-R4, or UNC45A and cultured in LGD1069 (bexarotene; 1 μmol/L) to allow for growth arrest to occur.

Published OnlineFirst October 20, 2009; DOI: 10.1158/1541-7786.MCR-09-0187

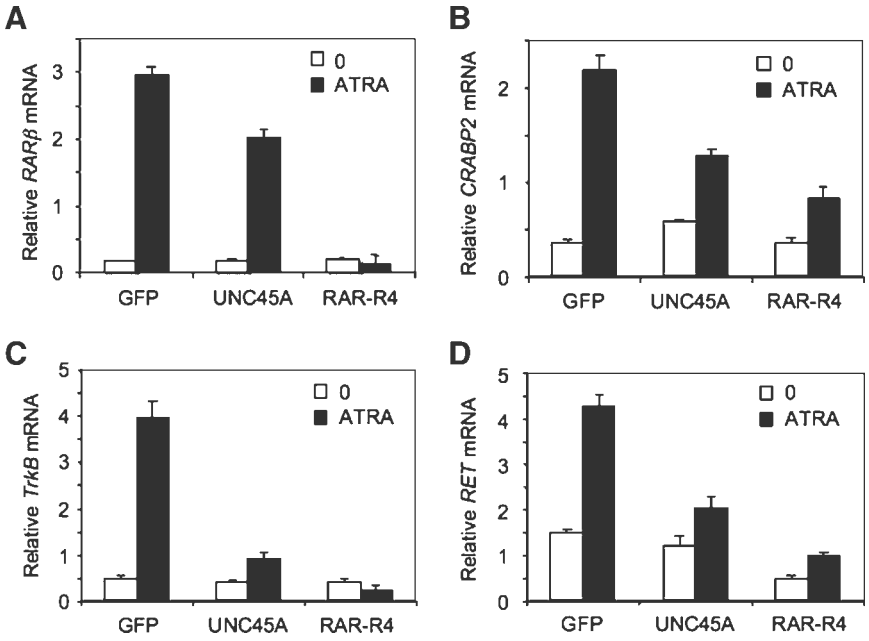

FIGURE 7. UNC45A inhibits ATRA-induced gene transcription. **A** and **B.** mRNA expression analysis of RA target genes *RARβ* and *CRABP2* in SH-SY-5Y cells expressing GFP, RAR-R4, or UNC45A after 3 wk in ATRA (0.1 μmol/L). **C** and **D.** mRNA expression analysis of neural differentiation markers *TRKB* and *RET* in SH-SY-5Y cells expressing GFP, RAR-R4, or UNC45A after 3 wk in ATRA (0.1 μmol/L).

cells were lysed in lysis buffer [50 mmol/L Tris (pH 7.5), 10% glycerol, 5 mmol/L $MgCl_2$, 75 mmol/L NaCl, 0.2% NP40, protease inhibitor cocktail EDTA-free (Complete, Roche), NaF, 0.2 mmol/L Na_3VO_4, 2.5 mmol/L sodium pyrophosphate, and 2.5 mmol/L sodium β-glycerophosphate] for 30 min and the lysates were centrifuged and incubated with anti-FLAG M2 agarose gel (Sigma). The immunoprecipitates were washed with wash buffer [50 mmol/L Tris (pH 7.5), 5 mmol/L $MgCl_2$, 75 mmol/L NaCl, 0.1% NP40, protease inhibitor cocktail EDTA-free (Complete, Roche), NaF, 0.2 mmol/L Na_3VO_4, 2.5 mmol/L sodium pyrophosphate, and 2.5 mmol/L sodium β-glycerophosphate] and eluated in 160 ng/μL 3Xflag peptide (Sigma) in wash buffer. The eluates were incubated with streptavidin magnetic beads (NEB Labs), the precipitates were washed with wash buffer and separated on Bis-Tris gradient gels (NuPAGE Novex, Invitrogen). The gels were stained with SimplyBlue dye (Invitrogen) and bands were cut out for in-gel trypsinization and analysis in a liquid chromatography tandem mass spectrometry spectrophotometer.

Disclosure of Potential Conflicts of Interest

No potential conflicts of interest were disclosed.

Acknowledgments

We thank Drs. Sidong Huang and Michael Hölzel for helpful suggestions and comments.

References

1. Barral JM, Bauer CC, Ortiz I, Epstein HF. Unc-45 mutations in Caenorhabditis elegans implicate a CRO1/She4p-like domain in myosin assembly. J Cell Biol 1998;143:1215–25.

2. Venolia L, Waterston RH. The unc-45 gene of Caenorhabditis elegans is an essential muscle-affecting gene with maternal expression. Genetics 1990;126:345–53.

3. Price MG, Landsverk ML, Barral JM, Epstein HF. Two mammalian UNC-45 isoforms are related to distinct cytoskeletal and muscle-specific functions. J Cell Sci 2002;115:4013–23.

4. Hutagalung AH, Landsverk ML, Price MG, Epstein HF. The UCS family of myosin chaperones. J Cell Sci 2002;115:3983–90.

5. Barral JM, Hutagalung AH, Brinker A, Hartl FU, Epstein HF. Role of the myosin assembly protein UNC-45 as a molecular chaperone for myosin. Science 2002;295:669–71.

6. Etard C, Behra M, Fischer N, Hutcheson D, Geisler R, Strahle U. The UCS factor Steif/Unc-45b interacts with the heat shock protein Hsp90a during myofibrillogenesis. Dev Biol 2007;308:133–43.

7. Wohlgemuth SL, Crawford BD, Pilgrim DB. The myosin co-chaperone UNC-45 is required for skeletal and cardiac muscle function in zebrafish. Dev Biol 2007;303:483–92.

8. Hoppe T, Cassata G, Barral JM, et al. Regulation of the myosin-directed chaperone UNC-45 by a novel E3/E4-multiubiquitylation complex in C. elegans. Cell 2004;118:337–49.

9. Landsverk ML, Li S, Hutagalung AH, et al. The UNC-45 chaperone mediates sarcomere assembly through myosin degradation in Caenorhabditis elegans. J Cell Biol 2007;177:205–10.

10. Chadli A, Felts SJ, Toft DO. GCUNC45 is the first Hsp90 co-chaperone to show α/β isoform specificity. J Biol Chem 2008;283:9509–12.

11. Chadli A, Graham JD, Abel MG, et al. GCUNC-45 is a novel regulator for the progesterone receptor/hsp90 chaperoning pathway. Mol Cell Biol 2006;26:1722–30.

12. Bazzaro M, Santillan A, Lin Z, et al. Myosin II co-chaperone general cell UNC-45 overexpression is associated with ovarian cancer, rapid proliferation, and motility. Am J Pathol 2007;171:1640–9.

13. Minucci S, Pelicci PG. Histone deacetylase inhibitors and the promise of epigenetic (and more) treatments for cancer. Nat Rev Cancer 2006;6:38–51.

14. Epping MT, Wang L, Plumb JA, et al. A functional genetic screen identifies retinoic acid signaling as a target of histone deacetylase inhibitors. Proc Natl Acad Sci U S A 2007;104:17777–82.

15. Epping MT, Bernards R. Molecular basis of the anti-cancer effects of histone deacetylase inhibitors. Int J Biochem Cell Biol 2009;41:16–20.

16. Epping MT, Wang L, Edel MJ, Carlee L, Hernandez M, Bernards R. The human tumor antigen PRAME is a dominant repressor of retinoic acid receptor signaling. Cell 2005;122:835–47.

17. Heery DM, Kalkhoven E, Hoare S, Parker MG. A signature motif in transcriptional co-activators mediates binding to nuclear receptors. Nature 1997;387:733–6.

18. Torchia J, Rose DW, Inostroza J, et al. The transcriptional co-activator p/CIP binds CBP and mediates nuclear-receptor function. Nature 1997;387:677–84.

19. Reynolds CP, Schindler PF, Jones DM, Gentile JL, Proffitt RT, Einhorn PA. Comparison of 13-*cis*-retinoic acid to *trans*-retinoic acid using human neuroblastoma cell lines. Prog Clin Biol Res 1994;385:237–44.

Published OnlineFirst October 20, 2009; DOI: 10.1158/1541-7786.MCR-09-0187

20. Sidell N, Altman A, Haussler MR, Seeger RC. Effects of retinoic acid (RA) on the growth and phenotypic expression of several human neuroblastoma cell lines. Exp Cell Res 1983;148:21–30.

21. Reynolds CP, Matthay KK, Villablanca JG, Maurer BJ. Retinoid therapy of high-risk neuroblastoma. Cancer Lett 2003;197:185–92.

22. Matthay KK, Villablanca JG, Seeger RC, et al, Children's Cancer Group. Treatment of high-risk neuroblastoma with intensive chemotherapy, radiotherapy, autologous bone marrow transplantation, and 13-*cis*-retinoic acid. N Engl J Med 1999;341:1165–73.

23. Esposito CL, D'Alessio A, de Franciscis V, Cerchia L. A cross-talk between TrkB and Ret tyrosine kinases receptors mediates neuroblastoma cells differentiation. PLoS ONE 2008;3:e1643.

24. Kaplan DR, Matsumoto K, Lucarelli E, Thiele CJ, Eukaryotic Signal Transduction Group. Induction of TrkB by retinoic acid mediates biologic responsiveness to BDNF and differentiation of human neuroblastoma cells. Neuron 1993;11:321–31.

25. Peterson S, Bogenmann E. The RET and TRKA pathways collaborate to regulate neuroblastoma differentiation. Oncogene 2004;23:213–25.

26. Coffey DC, Kutko MC, Glick RD, et al. The histone deacetylase inhibitor, CBHA, inhibits growth of human neuroblastoma xenografts *in vivo*, alone and synergistically with all-trans retinoic acid. Cancer Res 2001;61:3591–4.

27. Wang XF, Qian DZ, Ren M, et al. Epigenetic modulation of retinoic acid receptor β2 by the histone deacetylase inhibitor MS-275 in human renal cell carcinoma. Clin Cancer Res 2005;11:3535–42.

28. Kortlever RM, Higgins PJ, Bernards R. Plasminogen activator inhibitor-1 is a critical downstream target of p53 in the induction of replicative senescence. Nat Cell Biol 2006;8:877–84.

29. de Boer E, Rodriguez P, Bonte E, et al. Efficient biotinylation and single-step purification of tagged transcription factors in mammalian cells and transgenic mice. Proc Natl Acad Sci U S A 2003;100:7480–5.

AACR American Association for Cancer Research

Molecular Cancer Research

UNC45A Confers Resistance to Histone Deacetylase Inhibitors and Retinoic Acid

Mirjam T. Epping, Lars A.T. Meijer, Johannes L. Bos, et al.

Mol Cancer Res 2009;7:1861-1870. Published OnlineFirst October 20, 2009.